Study on the Control Effect of Viscoelastic Anti-Dancing Device on Long-span High-voltage Transmission Line under Icing Conditions

Guangxun Li[1], Qing Liu[1*], Xingyuan Qin[1], Manjia Ruan[1], Xu Deng[1], Yiting Li[1], Xun Deng[1], Xuemei Pan[1], Kabir Md Bourhan[2]

[1] Bijie Power Supply Bureau, Guizhou Power Grid Corporation, Bijie 551700, Guizhou, China
[2] School of civil engineering, Southeast University, Nangjing 211189, Jiangsu, China
[*] Corresponding author, 271070837@qq.com
DOI: 10.32629/aes.v5i4.3213

Abstract: This study investigates the control effect of a viscoelastic anti-dancing device on long-span high-voltage transmission lines subjected to icing conditions. The growing frequency of icing on transmission lines presents significant risks, including structural damage and service interruptions. The viscoelastic anti-dancing device aims to mitigate the negative impacts of dynamic oscillations induced by wind and ice accumulation. Through a combination of field tests and numerical simulations, the device's performance is assessed in terms of its ability to reduce vibration amplitudes and enhance the stability of transmission lines. Results demonstrate a marked improvement in oscillation control, leading to increased reliability and safety of high-voltage power transmission during adverse weather conditions. This research offers valuable insights into the use of viscoelastic materials for designing protective devices for transmission lines.
***Keywords*:** viscoelastic anti-dancing device, high-voltage transmission line, icing conditions, wind load simulation, structural stability, vibration control

1. Introduction

Transmission line dancing refers to a kind of low-frequency, large-amplitude self-excited vibration generated by non-circular cross-section transmission lines under the action of wind. Its vibration frequency is generally 0.1~5Hz, and the amplitude is 5~300 times the diameter of the transmission line [1-3]. The icing, wind excitation, and structural parameters of a transmission line significantly contribute to the phenomenon known as transmission line dancing.

Icing is a severe natural disaster of electrical power transmission lines. It will cause losses to the transmission systems in many aspects and bring serious threats to power system stability and even human energy security. In 1932, the United States recorded the first accident caused by icing on overhead lines in human history [4-5].

The icing galloping of transmission lines is not only affected by the icing load, but also other influencing factors such as wind [6-7], tower line system [8], and so on [9-11]. In the dynamic simulation analysis of transmission line ice-shedding, Hou et al. [12] developed a 3 degree of freedom (DOF) multi-level wire model suitable for analyzing transmission line ice-shedding and obtained its time response characteristics. Liang [13] studied transmission line ice-shedding under six ice-shedding rates and wind speeds. Wu [14] proposed a theoretical algorithm for the maximum ice-shedding and vibration height of transmission lines. Zhao et al. [15] studied the dynamic response characteristics of transmission line ice-shedding using finite-element numerical simulation. Xu [16] developed a finite-element model of a tower line coupling system and analyzed the dynamic response characteristics of transmission line ice-shedding. Yan et al. [17] analyzed transmission line ice-shedding and vibration amplitude under different wind speeds, spans, heights, insulator string lengths, numbers of tension sections, and other parameters.

This paper explores the mechanical properties and performance of a viscoelastic anti-dancing device under varying displacement amplitudes and frequencies. Through performance testing, the study reveals how the device's dynamic properties change with different loading conditions. A genetic algorithm is also developed for parameter optimization process was conducted using MATLAB. The anti-dancing effect is assessed via mid-span displacement responses, contributing valuable insights for improving transmission line stability in dynamic conditions.

2. Description of viscoelastic anti-dancing device

The viscoelastic anti-dancing device used in the test consists of an inner cylinder, a lower cover, a viscoelastic material, and a top cover. Figure 1 illustrates the viscoelastic anti-dancing device, and Calculated area of viscoelastic layer 2262 and 5027 (mm^2), viscoelastic layer thickness 20 and 30 (mm), viscoelastic layer radius 40 and 60 (mm), number of viscoelastic

layers 1&2 its design parameters.

Figure 1. Viscoelastic anti-dancing device

2.1 Viscoelastic anti-dancing device working system

The lower end of the transmission line spacer is fitted with a viscoelastic anti-dancing device. When the transmission line sways due to wind loads, the anti-dancing device on the spacer rod moves in sync. The inner cylinder and viscoelastic material create relative motion, generating an energy dissipation effect. Additionally, during the transmission line's movement, the entire anti-dancing device produces an inertial force that opposes the line's motion. This inertial force also helps control the transmission line's displacement response, functioning similarly to a TMD (tuned mass damper) effect.

2.2 Purpose of the trial of viscoelastic anti-dancing device

The mechanical properties test was conducted to determine the mechanical characteristics of the viscoelastic anti-dancing device. This test took place in the fall at room temperature (20–30 degrees Celsius) and examined the relationship between frequency, displacement amplitude, and the vibration damping ability of the device. By analyzing the dynamic mechanical properties of the resulting device, we evaluated its vibration damping capability.

2.3 Properties and characteristics of viscoelastic materials

The mechanical properties of viscoelastic dampers are defined by the stress-strain relationship of the viscoelastic material, which dissipates vibrational energy through hysteresis. Viscoelastic materials possess both viscous and elastic qualities, exhibiting mechanical characteristics that lie between those of viscous liquids and elastic solids. The energy storage modulus is frequently used in materials science G_1 to measure its energy storage characteristics G_2 , and its energy dissipation characteristics η are measured by the loss modulus or loss factor $\eta = G_2 / G_1$, as shown in equation (1), where τ represents the stress. When deformed by alternating stress, a portion of the energy is stored as potential energy, and the remaining portion is converted into heat energy consumption and dissipated. γ stands for the amplitude of strain.

$$\tau = G_1\gamma + G_2\dot{\gamma} \tag{1}$$

3. Mathematical model of transmission lines with and without viscoelastic anti-dancing device

To establish a theoretical basis for the practical application of the anti-dancing device in transmission line structures, a viscoelastic anti-dancing device is integrated into the ice-covered four-split transmission line structure. Motion equations and a calculation model are developed for this purpose. Current literature often estimates wind loads using a constant average wind speed, which does not accurately reflect real-world conditions. Therefore, it is essential to generate a time-varying wind load for calculating dancing effects.

3.1 Anti-dance dynamic model of ice-covered four-split transmission line structure

The split transmission line is a method used for erecting high-voltage transmission lines to minimize corona discharge and reduce line reactance. In this method, each phase of the transmission line consists of 2 ~ 4 smaller sub-transmission lines, which have a smaller diameter. The quadruple-split transmission line is primarily employed for 500 kV ultra-high voltage transmission lines, as illustrated in Figure 2.

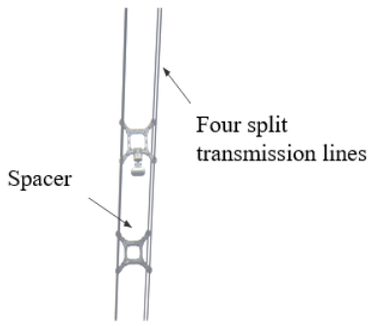

Figure 2. Quadruple split transmission line structure

The equation of motion is established as its mechanical model, as shown in Figure 3.The cross-section of any sub-transmission line within the ice-covered quadruple split transmission line structure is depicted in Figure 4(a). This figure utilizes a local coordinate system (y-C-z) to describe the motion state of the sub-transmission line, with C representing the torsion center. In Figure 3-3(b), the overall cross-section of the ice-covered four-split transmission line is illustrated, employing a global coordinate system (Y-O-Z) to describe the motion state of the equivalent single transmission line. The parameters Vi, Wi, and Θi denote the crosswind direction (Y direction) for each transmission line i (i = 1~4). Similarly, the displacements for the three degrees of freedom in the downwind direction (Z direction) and torsional direction are represented by V, W, and Θ, corresponding to the equivalent single transmission line.

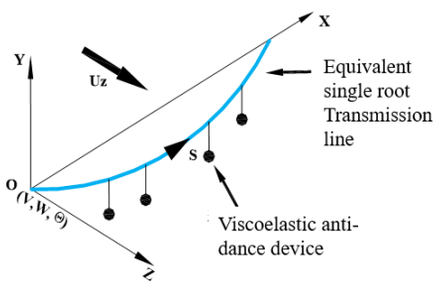

Figure 3. Equivalent single transmission line structure model

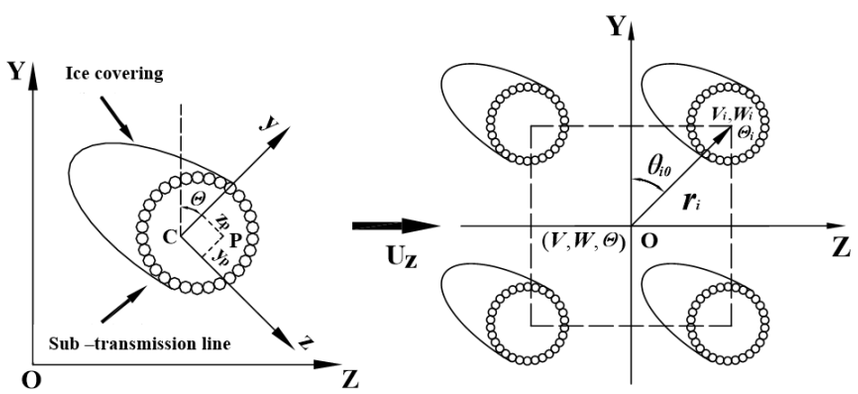

Figure 4. Cross-section of the ice-covered transmission line structure

As shown in Figure 3-3(a), if any point P on the ice-covered sub-transmission line is (zp, yp) in the local coordinate system, and the rotation angle of the dynamic coordinate system is Θ, the coordinates of the point in the global fixed coordinate system are:

$$\begin{aligned} Z_p &= Z + z_p \cos\Theta + y_p \sin\Theta \\ Y_p &= Y + y_p \cos\Theta - z_p \sin\Theta \end{aligned} \tag{2}$$

When Θ is small enough, equation (2) can be approximated as:

$$\begin{aligned} Z_p &= Z + z_p + y_p\Theta \\ Y_p &= Y + y_p - z_p\Theta \end{aligned} \tag{3}$$

By replacing Y and Z in equation (3) with the corresponding displacements V and W, the displacement relationship between the sub-transmission line in Article i and the equivalent single transmission line can be deduced, that is:

$$\begin{aligned} V_i(s,t) &= V(s,t) - r_i \sin\theta_{i0}\Theta(s,t) \\ W_i(s,t) &= W(s,t) + r_i \cos\theta_{i0}\Theta(s,t) \\ \Theta_i(s,t) &= \Theta(s,t) \end{aligned} \tag{4}$$

where is the ri distance between the center of the i-th sub-transmission line and the equivalent single transmission line, and θi0 is the clockwise angle between the center of the i-th sub-transmission line and the Y-axis.

3.2 Equation of motion for anti-dancing of ice-covered quadruple split transmission line structure

As a continuous system, the displacement of the transmission line structure depends not only on time but also on spatial coordinates. Therefore, the discrete method is chosen as the hypothetical mode method. In this context, the time-dependent aspect of the displacement is expressed as generalized displacement, while the spatial aspect is represented as the vibration mode.

Dividing the displacement in all directions at any point on an equivalent single transmission line as the product of the generalized displacement and the vibration mode yields:

$$V(s,t) = q_v(t) f_v(s)$$

$$W(s,t) = q_w(t) f_w(s) \tag{5}$$

$$\Theta(s,t) = q_\theta(t) f_\theta(s)$$

where $q_v(t)$, $q_w(t)$, $q_\theta(t)$ the generalized displacements in the crosswind, downwind, and torsional directions, respectively, $f_v(s)$, $f_w(s)$, $f_\theta(s)$ the vibration modes in the corresponding directions.

Based on the idea of energy analysis, the Lagrangian equation of dynamic equilibrium established:

$$\frac{d}{dt}\left(\frac{\partial T}{\partial \dot{q}_k}\right) - \frac{\partial T}{\partial q_k} + \frac{\partial V_s}{\partial \dot{q}_k} = Q_k \tag{6}$$

where T is the total kinetic energy of the iced transmission line, Vs is the potential energy of the iced transmission line, and q_k is the k-th generalized displacement, Q_k which is the corresponding non-conservative force.

The total kinetic energy T of the iced transmission line is expressed as:

$$T = \frac{1}{2}\int_0^L \int_{A_T} \left(\dot{Y}_p^{\,2} + \dot{Z}_p^{\,2}\right)\rho dA ds \tag{7}$$

where L is the full length of the transmission line, AT is the total area of the cross-section of the iced transmission line, and ρ is the density of a point on the cross-section of the iced transmission line. Substituting Eq. (3) into Eq. (7) and replacing Z and Y with the corresponding displacements V and W yield:

$$T = \int_0^L \left[\frac{1}{2}m\left(\dot{V}^2 + \dot{W}^2\right) + \frac{1}{2}J\dot{\Theta}^2 + S_z \cdot \dot{W}\dot{\Theta} - S_y \cdot \dot{V}\dot{\Theta}\right] ds \tag{8}$$

where , $m = \int_{A_T} \rho dA$ notes the mass of the iced transmission line per unit length; $J = \int_{A_T} \left({y_p}^2 + {z_p}^2 \right) dA$, which represents the moment of inertia of the iced transmission line per unit length; $S_z = \int_{A_T} y_p \rho dA$ which represents the mass moment $S_y = \int_{A_T} z_p \rho dA$ of the local coordinates of the ice-covered transmission line per unit length in the z and y axes respectively.

The total potential energy Vs of the iced transmission line is composed of the tensile strain energy, torsional strain energy and initial stress strain energy [24] of each strip transmission line, i.e.,

$$V_s = \sum_{i=1}^{4} \int_0^L [\frac{1}{2} AE {\varepsilon_s}^2 + \frac{1}{2} G {I_p} {\varepsilon_\theta}^2 + T_0 \varepsilon_s + M_0 \varepsilon_\theta]_i \, ds \tag{9}$$

where AE and GIp are the axial tensile stiffness and torsional stiffness of each iced transmission line, respectively, and T0 and M0 are the initial tensile force and initial torque of each iced transmission line, respectively ε_s ε_θ The axial strain and torsional strain of each iced transmission line are respectively denoted as:

$$\varepsilon_s = \frac{\partial Y}{\partial s}\frac{\partial V_i}{\partial s} + \frac{\partial Z}{\partial s}\frac{\partial W_i}{\partial s} + \frac{1}{2}\left[\left(\frac{\partial V_i}{\partial s} \right)^2 + \left(\frac{\partial W_i}{\partial s} \right)^2 \right]$$

$$\varepsilon_\theta = \frac{\partial \Theta}{\partial s} \tag{10}$$

where Y and Z are the coordinates of any point on the transmission line when the transmission line is at its initial position.

The aerodynamic loads of each ice-covered sub-transmission line per unit length in the crosswind direction, downwind direction and torsion direction are FY, FZ and Mθ respectively, and the formula is as follows:

$$F_Y = \frac{1}{2} \rho_{air} {U_z}^2 dC_y$$

$$F_Z = \frac{1}{2} \rho_{air} {U_z}^2 dC_z \qquad M_\theta = \frac{1}{2} \rho_{air} {U_z}^2 d^2 C_\theta \tag{11}$$

where is the ρ_{air} air density, U_z is the wind speed, d is the diameter of the transmission line C_y , C_z and C_θ are expressed as the aerodynamic coefficients of the cross-wind direction, downwind direction, and torsion direction, respectively, which are fitted by the experimental data, and the fitting curve [20]:

$$C_y = -0.6670\alpha - 16.2188\alpha^2 + 33.4324\alpha^3$$

$$C_z = 3.4420\alpha + 3.3300\alpha^2 + 7.1262\alpha^3$$

$$C_\theta = -2.9086\alpha + 1.1738\alpha^2 + 23.8816\alpha^3 \tag{12}$$

where $\alpha = \Theta - \frac{\dot{V}}{U_z} - \frac{d}{2U_z}\dot{\Theta}$ is the angle of attack of the wind load.

Substituting equations (8), (9), and (10) into equations (6) can obtain the equation of motion for the transmission line dance:

$$[M]\{\ddot{q}\} + [C]\{\dot{q}\} + [K]\{q\} = \{P\} \tag{13}$$

Where $\{q\}^T = \{q_v \ q_w \ q_\theta\}$; The forces exerted in the direction of the three degrees of freedom $\{P\}^T = \{P_Y \ P_Z \ P_\theta\}$, P_Y , P_Z are P_θ respectively expressed as:

$$P_Y = \sum_{i=1}^{4}\int_0^L f_v(s)\cdot F_Y ds - \sum_{i=1}^{4} H_0 \int_0^L \frac{\partial s}{\partial X}\frac{\partial Y}{\partial s}\frac{\partial f_v(s)}{\partial s} ds$$

$$P_Z = \sum_{i=1}^{4}\int_0^L f_w(s)\cdot F_Z ds - \sum_{i=1}^{4} H_0 \int_0^L \frac{\partial s}{\partial X}\frac{\partial Z}{\partial s}\frac{\partial f_w(s)}{\partial s} ds$$

$$P_\theta = \sum_{i=1}^{4}\int_0^L f_\theta(s)\cdot M_\theta ds - \sum_{i=1}^{4} M_0 \int_0^L \frac{\partial f_\theta(s)}{\partial s} ds$$

$$-\sum_{i=1}^{4} H_0 \int_0^L r_i \cdot \left(\frac{\partial Z}{\partial s}\frac{\partial f_\theta(s)}{\partial s}\cos\theta_{i0} - \frac{\partial Y}{\partial s}\frac{\partial f_\theta(s)}{\partial s}\sin\theta_{i0}\right) ds \tag{14}$$

In Eq. (13), $[M]$, and $[C]$, respectively, are the mass matrix, the damping matrix, and the stiffness matrix.

The model of the viscoelastic anti-dancing device suspended at the spacer rod of the four-split transmission line can refer to the mechanical model of adding TMD in the building structure[26], and only the TMD force acting on the crosswind direction is considered, and the crosswind displacement of the viscoelastic anti-dancing device is also written as the product of the generalized displacement and the vibration mode, that is:

$$V_{vdj}(s_j, t) = q_{vdj}(t) f_{vdj}(s_j) \tag{15}$$

In the formula, $V_{vdj}(s_j, t)$ which is the crosswind displacement of the j-th anti-dancing device $q_{vdj}(t)$ and $f_{vdj}(s_j)$ the generalized displacement and vibration mode of the j-th anti-dancing device, respectively, and then using the Lagrangian equation of Eq. (3-5), it can be deduced that the dynamic balance equation of the transmission line becomes after adding the viscoelastic anti-dancing device

$$m_{dj} f_{vdj}(s_j)\ddot{q}_{vdj}(t) + c_{dj}\left[f_{vdj}(s_j)\dot{q}_{vdj}(t) - f_v(s)\dot{q}_v(t)\right] + k_{dj}\left[f^2{}_{vdj}(s_j) q_{vdj}(t) - f_v^2(s) q_v(t)\right] = 0 \tag{16}$$

In Eq (18), $\ddot{q}_{vdj}(t)$, $\dot{q}_{vdj}(t)$ the generalized acceleration of the j-th anti-dancing device, respectively, velocity, m_{dj} , c_{dj} , k_{dj} the mass, damping, and stiffness of the j-th anti-dancing device are respectively, and the meaning of the other parameters is the same as above.

Different the forced vibration experienced by structures during seismic events, the oscillation of iced transmission line structures is classified as self-excited vibration. In a forced vibration system, energy is received solely from external sources during the vibration process. In contrast, a self-excited vibration system can independently draw energy from its energy source and uses its own motion state as a regulator to adjust the energy input through feedback. The equation of motion for the iced transmission line structure is solved based on this principle, as illustrated in Figure 5. Under the influence of the initial, Θ , and other parameters of the $\dot{V}$ transmission line structure $\dot{\Theta}$, when the wind speed is U_z the wind load, the angle of attack is generated α . The αaerodynamic coefficient can be obtained C_y , C_z and C_θ the load in the downwind, crosswind, and torsion directions of the transmission line structure can be obtained. Under the action of load, the transmission line structure undergoes downwind, crosswind, and torsional movements, and produces a new state of movement Θ , $\dot{V}$ and $\dot{\Theta}$ then feeds back the wind load again, so that the process starts again and again, and the cycle repeats. The calculation process can be analyzed by using MATLAB with reference to the Newmark-β method.

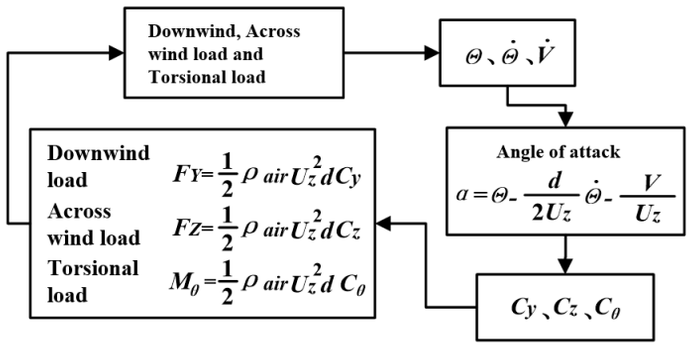

Figure 5. Iced transmission line structure dancing process

3.3 Analysis of anti-dancing response of icing quadruple split transmission line structure

The kinetic model outlined in this conte is employed to evaluate the dynamic response of an iced quadruple split transmission line structure's anti-dancing behavior, supported by a case study. Table 1 presents the parameters for the ice-covered transmission line structure utilized in this example. Each device has a mass of m_d = 10 kg and a natural frequency of ω_d = 24.50 rad/s. The horizontal distances from the origin O to each of the four anti-dancing devices are s_1 = 20 m, s_2 = 60m, s_3 = 80m, and s_4 = 100m respectively.

Table 1. Structural parameters of iced transmission lines

Parameter	Numeric value	Parameter	Numeric value
Transmission line diameter d(m)	0.0286	Transmission line span L(m)	800
Transmission line cross-sectional area A (m^2)	423.24	Cross-sectional area of icing on the transmission line Aice(m^2)	171.24
Modulus of elasticity of power transmission lines E(N/m^2)	4.78033×10^{10}	Horizontal tension of power transmission line H (N)	30000
Torsional stiffness of power lines GIp (Nm^2/rad)	101	Iced transmission line unit mass m (kg/m)	2.379
Air density ρ_{air} (kg/m^3)	1.2929	The distance between the transmission line and the equivalent line ri(m)	0.2355
Transmission line torsion-to-damping ratio ξ_θ	0.308	Transmission line crosswind direction, downwind direction damping ratio ξ_y , ξ_z	0.515×10^{-3}
Transmission line unit mass moment Sy(kg)	0.266×10^{-3}	Transmission line unit mass moment Sz (kg)	0.266×10^{-3}

In the dance response of the transmission line structure, the mid-span displacement response is a critical factor. Therefore, the mid-span displacement response of the iced transmission line structure is calculated and compared in the downwind, crosswind, and torsional directions for both uncontrolled and controlled states.

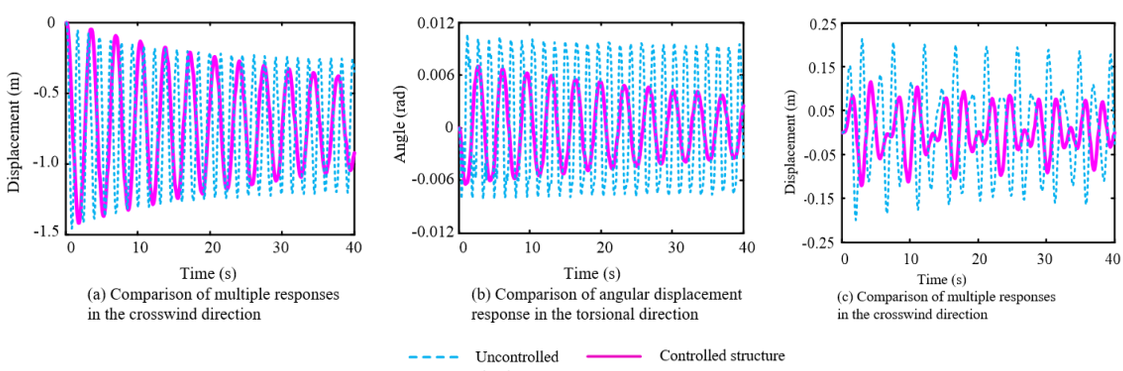

Figure 6. The uncontrolled and most controlled structures have displacement responses in all directions across the span.

As shown in Figure 6, the mid-span displacement response of the transmission line structure in the downwind, crosswind, and torsion directions is reduced compared with the uncontrolled state when the viscoelastic anti-dancing device is

added, indicating that the viscoelastic anti-dancing device plays a certain role in controlling the dancing of the transmission line structure.

4. Conclusion

The study demonstrates that the implementation of viscoelastic anti-dancing devices significantly enhances the performance of long-span high-voltage transmission lines under icing conditions. According to the findings, these devices effectively reduce torsional and crosswind displacements, facilitating a transition from unstable, self-excited vibrations to a more stable state. This is achieved by disrupting the energy balance and minimizing the energy absorbed from wind loads, which is crucial for preventing structural damage during adverse weather conditions.

Quantitative results indicate remarkable attenuation rates, with torsional displacements decreasing by 96.7% and crosswind displacements by up to 97.0%. Additionally, there was a significant reduction in the downwind displacement response, leading to a more favorable energy state for the transmission line structure. The effectiveness of viscoelastic anti-dancing devices in mitigating vibration issues was evident in the significant reduction in energy consumption.

In conclusion, incorporating viscoelastic anti-dancing devices proves to be a practical and effective approach to enhancing the stability and durability of high-voltage transmission lines in challenging environmental conditions, ensuring reliable operation and reduced maintenance costs.

Acknowledgments

This paper sincerely appreciate the support by the 2024 Power Technology Development Project of Bijie Power Supply Bureau of Guizhou Power Grid Co., Ltd. (Project No.: 060700KC23120015).

References

[1] Guo Yinglong, Li Guoxing, You Chuanyong. Transmission line dance[M]. Beijing: China Electric Power Press.2003.
[2] ZHAO Zuoli. Transmission line dancing and its prevention and control[J].High Voltage Engineering, 2004, 30(2): 57-58.
[3] ZHANG Ping. Analysis of the causes of transmission line dancing and anti-dancing measures of overhead transmission lines[J].Electric Power Technology of Inner Mongolia, 2009, 27(5): 11-13.
[4] Imai, I. Studies on Ice Accretion. Res. Snow Ice 1953, 1, 35–44.
[5] Rossi, A., 2018. Wind Tunnel Modelling of Snow and Ice Effects on Transmission Lines. Technical University of Denmark.
[6] K. Natarajan and A. R. Santhakumar, ‘‘Reliability-based optimization of transmission line towers,’’ Comput. Struct., vol. 55, no. 3, pp. 387–403, May 1995.
[7] A. Kudzys, ‘‘Safety of power transmission line structures under wind and ice storms,’’ Eng. Struct., vol. 28, no. 5, pp. 682–689, Apr. 2006, doi: 10.1016/j.engstruct.2005.09.026.
[8] M. X. Zhao, B. He, and Y. Z. Feng, ‘‘Influence of coupling factors on mechanical property of high voltage transmission,’’ Proc. CSEE, vol. 38, no. 24, pp. 682–689, 2018, doi: 10.13334/j.0258-8013.pcsee.180473.
[9] G. A. Fenton and N. Sutherland, ‘‘Reliability-based transmission line design,’’ IEEE Trans. Power Del., vol. 26, no. 2, pp. 596–606, Apr. 2011,doi: 10.1109/TPWRD.2009.2036625.
[10] S. H. Wang, ‘‘Study on iced conductor galloping and influence on dynamic properties of transmission tower-line system,’’ Chongqing Univ., Chongqing, China, Tech. Rep., 2008.
[11] T. H. Xiong, J. G. Hou, and X. W. An, ‘‘Reliability analysis of a transmission tower in South China under ice load and wind load,’’ Eng. J. Wuhan Univ., vol. 44, no. 2, pp. 207–210, 2011.
[12] Hou, L.; Wang, L.; Zhu, P.; Guan, Z. Dynamic Behavior Computation of Ice Shedding of UHV Overhead Transmission Lines. Proc. Chin. Soc. Electr. Eng. 2008, 28, 1–6.
[13] Liang, C. Research on Ice Shedding from 220 kV-Double-Circle Transmission Line in Heavy Icing Area. Master’s Thesis, North China Electric Power University, Baoding, China, 2017.
[14] Wu, C. Study on Jump Height after Ice-shedding and Galloping Oscillation Characteristics of Transmission Lines. Ph.D. Thesis, Chongqing University, Chongqing, China, 2017.
[15] Zhao, Y.; Li, L.; Deng, W. Transmission lines ice-shedding numerical simulation jump-height after ice shedding horizontal amplitude. Water Res. Power 2013, 31, 211–215.
[16] Xu, G. Numerical Simulation Study of Iced Conductor on Dynamic Response of Ice-Shedding on Transmission Lines. Master’sThesis, Xi’an Technology University, Xi’an, China, 2016.
[17] Yan, B.; Chen, K.; Xiao, H.; Li, L.; Yi, W. Horizontal amplitude of iced conductor after ice-shedding under wind load. Chin. J. Appl. Mech. 2013, 30, 913–919.